This article was downloaded by:
On: *25 January 2011*
Access details: *Access Details: Free Access*
Publisher *Taylor & Francis*
Informa Ltd Registered in England and Wales Registered Number: 1072954 Registered office: Mortimer House, 37-41 Mortimer Street, London W1T 3JH, UK

Separation Science and Technology
Publication details, including instructions for authors and subscription information:
http://www.informaworld.com/smpp/title~content=t713708471

CHARACTERIZATION AND PROPERTIES OF SUPPORTED PROTEIN MEMBRANES

J. Bullón[a]; J. J. Chaffaut[a]; M. P. Belleville[a]; R. D. Newman[b]; G. M. Rios[a]
[a] Laboratoire des Matériaux et des Procédés Membranaires, Montpellier, Cedex 05, France [b] Department of Chemical Engineering, Auburn University, Alabama, U.S.A.

Online publication date: 11 September 2001

To cite this Article Bullón, J. , Chaffaut, J. J. , Belleville, M. P. , Newman, R. D. and Rios, G. M.(2001) 'CHARACTERIZATION AND PROPERTIES OF SUPPORTED PROTEIN MEMBRANES', Separation Science and Technology, 36: 14, 3071 — 3089
To link to this Article: DOI: 10.1081/SS-100107760
URL: http://dx.doi.org/10.1081/SS-100107760

PLEASE SCROLL DOWN FOR ARTICLE

Full terms and conditions of use: http://www.informaworld.com/terms-and-conditions-of-access.pdf

This article may be used for research, teaching and private study purposes. Any substantial or systematic reproduction, re-distribution, re-selling, loan or sub-licensing, systematic supply or distribution in any form to anyone is expressly forbidden.

The publisher does not give any warranty express or implied or make any representation that the contents will be complete or accurate or up to date. The accuracy of any instructions, formulae and drug doses should be independently verified with primary sources. The publisher shall not be liable for any loss, actions, claims, proceedings, demand or costs or damages whatsoever or howsoever caused arising directly or indirectly in connection with or arising out of the use of this material.

SEPARATION SCIENCE AND TECHNOLOGY, 36(14), 3071–3089 (2001)

CHARACTERIZATION AND PROPERTIES OF SUPPORTED PROTEIN MEMBRANES

J. Bullón,[1,2] J. J. Chaffaut,[1] M. P. Belleville,[1,*] R. D. Newman,[3] and G. M. Rios[1]

[1]Laboratoire des Matériaux et des Procédés Membranaires, Montpellier Cedex 05, France
[2]Laboratorio de Fenómenos Interfaciales y Recuperación de Petróleo, Universidad de Los Andes, Facultad de Ingeniería, Mérida 5101, Venezuela
[3]Department of Chemical Engineering, Auburn University, Alabama, USA

Downloaded At: 10:41 25 January 2011

ABSTRACT

Transport properties of a new type of filtering material, prepared by tangential filtration of a protein solution on a macroporous ceramic support, were determined. Retention characteristics were studied by filtration of polyethylene glycol solutions with various molecular weights at different pH and ionic strengths. The pore radii (1.5 nm) were estimated from pure water hydraulic permeability and reflection coefficients through the use of a theoretical model based on the Verniory pore theory. The protein layer morphology was examined by scanning electron and atomic force microscopy.

Key Words: Mass transfer; Characterization; Membrane; Cross-flow filtration; Protein

*Corresponding author. Fax: +33 (0)4 67149148; E-mail: Belleville@iemm.univ-montp2.fr

Copyright © 2001 by Marcel Dekker, Inc. www.dekker.com

ORDER REPRINTS

INTRODUCTION

Progress in membrane separation is closely linked to the development of membrane material. Since the 1960s, researchers in material science have undertaken studies to improve the properties of the membrane, such as its permeability and selectivity, its mechanical and thermal stability, and its chemical resistance. In the 1990s, the production of a wide range of material of different nature (organic/inorganic), with pore diameters ranging from 1 to 10 nm, permitted the development of new separation processes such as nanofiltration and low ultrafiltration.

For several years, researchers have been developing hybrid membranes elaborated from macromolecular deposits formed on ceramic supports during tangential filtration of protein solutions. Thus Negrel et al. (1,2) reported the preparation of a very low-ultrafiltration membrane (approximate M.W. of 2000 d) by cross-flow filtration of a gelatin solution over a 0.2 μm-pore cylindrical α-alumina support. The deposited layer was then hardened and tightened by chemical (tanning) and physical (thermal drying) treatments. In 2000, Bullón, Belleville, and Rios (3) optimized this manufacturing procedure by lowering the total time of preparation of 5 hours to less than 2 hours and by reducing the pore size to obtain better retention. These membranes have the advantage of working under low transmembrane pressure. They are biocompatible, do not clog, are easy to prepare and regenerate, and present adjustable properties according to specific objectives. They constitute attractive potential candidates for the concentration and purification of biological and pharmaceutical solutions that are sensitive to high temperature and shear.

The objective of this study was to characterize the separation properties of such protein membranes. Transfer parameters (L_p,σ) were deduced from filtration experiments with calibrated polyethylene glycol (PEG) molecules and pore diameter was estimated through an approach developed by Nakao and Kimura (4). Membrane characterization was completed by use of scanning electron microscopy (SEM) and atomic force microscopy (AFM).

THEORETICAL BACKGROUND

In 1981, Nakao and Kimura (4) presented a model based on film theory, the equations of nonequilibrium thermodynamic and the pore theory, in an attempt to characterize ultrafiltration transport mechanisms. This model, which has been already used by Sarrade, Rios, and Carles (5) to determine the transport properties and pore diameters of two nanofiltration membranes, is briefly described.

In film theory, the transport parameters L_p (solvent permeability), σ (solute reflection coefficient), and ω (solute membrane permeability) are determined according to Kedem-Katchalsky equations (Eqs. 1 and 2) from the experimental

Downloaded At: 10:41 25 January 2011

Copyright © Marcel Dekker, Inc. All rights reserved.

MARCEL DEKKER, INC.
270 Madison Avenue, New York, New York 10016

ORDER REPRINTS

measurements of solvent (J_v) and solute (J_s) fluxes under various experimental conditions.

$$J_v = L_p(\Delta P - \sigma\Delta\Pi) \tag{1}$$

$$J_s = \omega\,(C_m - C_p) + (1 - \sigma)\,J_v C^* \tag{2}$$

More precisely L_p is experimentally estimated by filtrating ultrapure water ($\Delta\Pi = 0$) while ω and σ are attained through a graphical procedure in which $J_s/\Delta\ C$ vs. $J_v C^*/\Delta C$ and where C^* is the mean logarithmic concentration between the two faces of the membrane:

$$C^* = \left[\frac{C_m - C_p}{\ln \dfrac{C_m}{C_p}}\right] \tag{3}$$

C_m, the concentration of the solute at the inner membrane surface is obtained through the use of the film model described by Michaels (6) and modified by Porter (7).

$$J_v = k \ln\left[\frac{C_m - C_p}{C_o - C_p}\right] \tag{4}$$

where C_o and C_p are the solute concentrations in the feed and the permeate streams respectively, and k is the mass transfer coefficient between the fluid and the membrane wall. k can be estimated by means of a dimensional correlation, such as that by Deissler (8):

$$\mathrm{Sh} = 0.023 \cdot \mathrm{Re}^{0.75} \cdot \mathrm{Sc}^{075} \tag{5}$$

When retention is very high, $\Delta C = C_m - C_p$ and can be very large, and Eq. 3 is no longer valid. Equation (2) is substituted by Eq. (6):

$$R^* = \frac{\sigma(1 - F)}{1 - (\sigma F)} \tag{6}$$

in which

$$F = \exp\left[\frac{-J_v\,(1 - \sigma)}{\omega}\right] \tag{7}$$

and R^*, the real retention rate, is obtained through application of Eq. (8). This latter parameter is more characteristic of the effective membrane selectivity than the observed retention rate (R) calculated using Eq. (9) because the fluid-wall interface concentration, $C_{m,}$ exceeds $C_{o.}$

$$R^* = \left[\frac{C_m - C_p}{C_m}\right] \tag{8}$$

$$R = \left[\frac{C_o - C_p}{C_o}\right] \tag{9}$$

Downloaded At: 10:41 25 January 2011

Copyright © Marcel Dekker, Inc. All rights reserved.

MARCEL DEKKER, INC.
270 Madison Avenue, New York, New York 10016

ORDER REPRINTS

The membrane pore radius r_p is related to the value of σ through the pore theory developed by Pappenheimer, Renkin, and Borrero (9) and modified by Verniory et al. (10) in the following manner:

$$(1 - \sigma) = \left[\frac{1 - 2/3q^2 - 0.2q^5}{(1 - 76q^5)}\right][2(1 - q)^2 - (1 - q)^4] \tag{10}$$

where

$$q = \frac{r_s}{r_p} \tag{11}$$

From knowledge of r_s, one can calculate the solute radius, r_p, by trial and error over q and by comparing the values of σ estimated either from drawings or from Eqs. (6) and (7).

MATERIAL AND METHODS

All the filtration experiments were performed on a small-scale pilot unit as shown in Fig. 1. The retentate and permeate streams were recycled and the operating conditions were $\Delta P = 0.2$ MPa, $U = 1$ m/s, and $T = 293$K.

Membrane Preparation and Characterization (Flux And Retention)

The protein membranes used in this study were prepared by depositing and stabilizing a gelatin layer on an inorganic tubular support as previously described (2,3). A 10 kg/m^3 of B type gelatin from Merck (France) was filtered for 25 min-

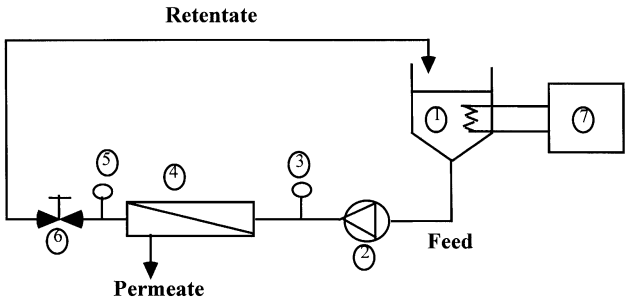

Figure 1. Pilot plant 1) feed tank, 2) pump, 3 and 5) pressure gauges, 4) membrane cartridge, 6) counterpressure valve, and 7) temperature control.

Downloaded At: 10:41 25 January 2011

Copyright © Marcel Dekker, Inc. All rights reserved.

MARCEL DEKKER, INC.
270 Madison Avenue, New York, New York 10016

ORDER REPRINTS

utes over an α-alumina macroporous substrate (0.2 μm) from US Filter (Tarbes, France). Then the dynamic protein deposit was treated with a formaldehyde solution (30 minutes with 5% formaldehyde solution at 293K) and dehydrated at 383K for 45 minutes.

The membrane permeability and selectivity were estimated by carrying out standardized filtration experiments with pure water and 15 kg/m^3 aqueous solutions of PEG (Merck) with different M.W. values: 0.6, 1.5, and 6.0 kd. The PEG concentrations were determined through the use of a differential refractometer (Shimadzu RID-6A model).

Volume fluxes (l/h·m^2) and retention yields R (%) thus obtained did not allow us to affirm that the protein-layer modifications are due to PEG adsorption or deposition. Several runs performed successively with the same membrane provided the same retention data; water fluxes measured before and after PEG filtration were identical.

Downloaded At: 10:41 25 January 2011

Membrane Transport Properties

The determination of membrane transport properties involved four different PEG solutions of M.W. 0.4, 0.6, 1.0, and 1.5 kd respectively. To prevent any problem of microbial contamination, sodium azide (0.2 kg/m^3) was added to the PEG solutions. Because different PEG concentrations (from 15 to 105 kg/m^3) were tested, diffusivities and kinematic viscosities of PEG solutions are reported in Table 1. These values were found in the literature or calculated from other data (5). Solutions with different concentrations were filtered and permeate flux/concentrations were measured at the steady state (generally reached after 10 or 15 minutes of filtration). After each test, the membrane was either rinsed with pure

Table 1. Diffusion Coefficients (D) and Kinematic Viscosities (υ) of Different PEG Solutions

	$(D)(10^{-10}$ m^2/s)			$(\upsilon)(10^{-6}$ m^2/s)		
C_o (kg/m^3)	PEG 0.6 kd	PEG 1.0 kd	PEG 1.5 kd	PEG 0.6 kd	PEG 1.0 kd	PEG 1.5 kd
15	4.0	2.9	2.2	1.2	1.2	1.3
30	3.2	2.4	1.7	1.5	1.6	1.6
45	2.6	1.9	1.3	1.8	2.0	2.1
60	2.2	1.5	1.0	2.2	2.5	2.7
75	1.8	1.2	0.8	2.6	3.1	3.5
90	1.4	1.0	0.6	3.3	4.0	4.6
105	1.2	0.8	0.5	4.1	5.0	5.9

Copyright © Marcel Dekker, Inc. All rights reserved.

MARCEL DEKKER, INC.
270 Madison Avenue, New York, New York 10016

ORDER REPRINTS

water before another test or removed using a classical cleaning procedure already described elsewhere (2).

Effect of Solution pH and Ionic Strength

To examine the evolution of protein membrane characteristics as a function of pH and ionic strength of solutions, the following complementary studies were completed.

Effect of pH

The membrane retention was estimated as a function of pH for the values of 2.0, 6.5, and 9.0. The intermediate value 6.5 corresponds to the pH of PEG solutions prepared with ultrapure water. pH was regulated by adding NaOH or HNO_3 from 0.1 mol/L solutions. The change of ionic strength due to pH control (from 10^{-3} to 2.10^{-3} mol/L) was low enough to avoid significant linked effects. First, the membrane was hydrated by filtrating ultrapure water at the desired pH value for 1 hour. Then, the solutions of PEG 0.6, 1.5, and 6.0 kd, each at a concentration of 15 kg/m^3 and a pH adjusted to the desired value, were filtered successively. After the filtration of each PEG solution, the membrane was rinsed with water at the desired pH. Finally, it was washed with ultrapure water for 2 hours and characterized according to the standardized procedure described under Membrane Preparation and Characterization.

Effect of Ionic Strength

The effect of ionic strength on flux and retention was studied using NaCl solutions at concentrations of 0.02, 0.20, and 1.00 mol/L. The experimental protocol was similar to the one previously described for pH effects. The membrane was hydrated with water at the desired NaCl concentration. The solutions of PEG (15 g/L) with NaCl were then filtered. Then, each PEG filtration membrane was washed with a NaCl solution at the desired concentration.

Physical Characterization

The SEM observations were performed on an Hitachi S4500 microscope. The samples of the membranes were previously dried in vacuum and covered with graphite for their protection.

The AFM used in the present study was a Nanoscope II (Version 4.22), from Digital Instruments, equipped with a silicon stylus model FESP that is 225 μm

Downloaded At: 10:41 25 January 2011

Copyright © Marcel Dekker, Inc. All rights reserved.

Marcel Dekker, Inc.
270 Madison Avenue, New York, New York 10016

ORDER REPRINTS

long. The measurements did not require any preparation of the samples and were made either in air or in water when the Nanoscope was operating in noncontact mode (taping mode).

RESULTS AND DISCUSSION

Effect of pH and Ionic Strength of Solutions

As previously reported in the literature (11–15), the hydraulic resistance of the protein deposit is a function of the pH and ionic strength that reflects both the inter- and intramolecular electrostatic interactions between the protein molecules within the deposit. The effect of these two variables over the flux and the retention of gelatin membrane during filtration of PEG solutions was studied.

The results obtained for experimental runs conducted at pH 2.0, 6.5, and 9.0 are shown in Fig. 2. The fluxes of the PEG solutions at a pH 2.0 are twice as high as those at pH 6.5. The difference between pH 6.5 and 9.0 is less marked, being a little higher at basic pH values. The evolution of the retention versus pH is con-

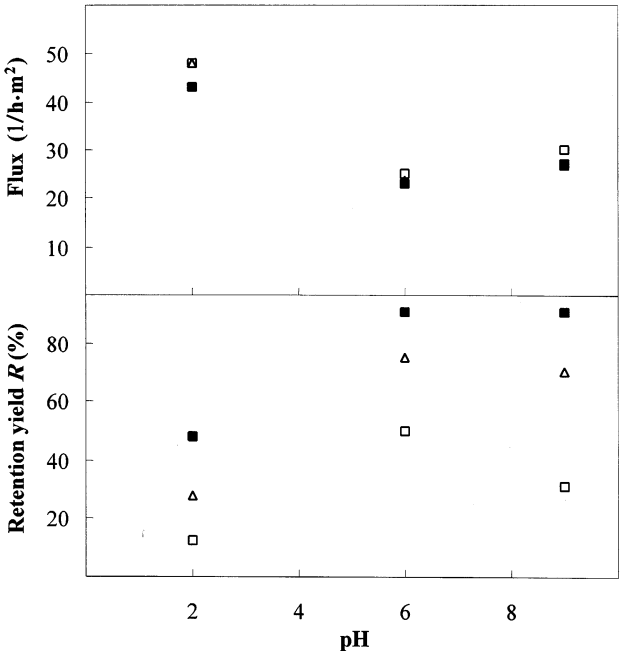

Figure 2. Flux and retention yields versus pH (□ PEG 0.6 kd, △ PEG 1.5 kd, ■ PEG 6.0 kd).

Downloaded At: 10:41 25 January 2011

Copyright © Marcel Dekker, Inc. All rights reserved.

MARCEL DEKKER, INC.
270 Madison Avenue, New York, New York 10016

ORDER REPRINTS

sistent with the fluxes obtained. The retentions are 2 to 3 times higher at pH 6.0 than they are at pH 2.0. The values obtained at pH 9.0 are of the same order as those obtained at pH 6.5 in the case of PEG 6.0 kd and a little less in the case of PEG 1.5. kd. For the PEG 0.6 kd, the retention diminishes for pH values over 6.0.

Thus the pH has a strong influence on the gelatin membrane structure. The membrane pores all seem to become larger at acid pH values (higher fluxes and less retention). At basic pH values, the molecular weight cut off (MWCO) of the membrane seems to be unmodified (nearly constant flux and retention of higher PEG M.W.), but the membrane pore distribution is probably more disperse: The proportion of pores that let the PEG 0.6 kd pass through the membrane increases. Huisman, Prádanos, and Hernández (16) found similar results. They presented AFM images of membranes fouled with proteins at different pH values. The more open structure was obtained at low pH.

The phenomenon observed is probably linked to protein morphologic changes. In highly acidic conditions, gelatin undergoes a transformation from a collagen-like structure to a more random-coil-like structure (17), which would explain the large changes in flux at pH 2. As this reaction does not occur to the same extent at pH 9, more subtle conformational transformations are most likely responsible for the observed permeability changes.

Furthermore, the affect of pH on protein charge must be taken into account. At pH 6.5, 1 unit of pH above the isoelectric point, the membrane is slightly charged. The electrostatic repulsions between the protein chains are low and the membrane is more compact, which accounts for the lower fluxes and the higher retentions observed. In acid or basic media, the presence of positive (pH 2) or negative (pH 9) charges enhances the repulsion between the protein chains, generating a freer space to allow the passage of solvent and solutes.

To evaluate the reversibility of the pH effect, 1 membrane was tested at pH 2 and 9. After each experimental series, the membrane was subjected to 2-hour ultrapure water filtration and characterized through the standard procedure. Results are shown in Table 2 . In another set of experiments (Table 3), the protein mem-

Table 2. Standardized Characterization of a Protein Membrane Before and After Filtration of Acidic and Basic Solutions

	Retention Yield (%)		
kd	Initial	After Filtration at pH 2	After Filtration at pH 9
PEG 0.6	50	21	19
PEG 1.5	75	55	46
PEG 6.0	91	85	85

Downloaded At: 10:41 25 January 2011

Copyright © Marcel Dekker, Inc. All rights reserved.

MARCEL DEKKER, INC.
270 Madison Avenue, New York, New York 10016

ORDER REPRINTS

Table 3. Standardized Characterization of a Protein Membrane Before and After Filtration of Basic and Acidic Solutions

	Retention Yields (%)			
kd	Initial	After Filtration at pH 9	After Rinsing (8 hours)	After Filtration at pH 2
PEG 0.6	50	34	39	28
PEG 1.5	75	65	68	58
PEG 6.0	91	92	92	87

brane was first tested at pH 9 and a second longer rinsing (8 hours of ultrapure water filtration) was carried out before pH 2 experiments were performed.

The results obtained show that whatever the pH conditions first tested, the retention characteristics of the membrane are affected; even a long rinsing time does not allow for the recovery of the original membrane properties. The use of the protein membrane in acidic conditions affects its structure in an irreversible manner and to a greater extent than does the basic pH. The retention values of PEG 0.6 and 1.5 kd are lowered at both pH 2 and pH 9, while the retention of PEG 0.6 kd is affected only at pH 2. Furthermore, after the membrane was treated at low or high pH, the retention characteristics were no longer affected by basic conditions; however, acidic pH still modified them.

The incidence of the ionic strength over the retention and permeate flux was also studied through successive filtrations of PEG solutions with increasing ionic concentration. The results are shown in Fig. 3. In presence of NaCl, the permeate fluxes are high for all PEG concentrations used. This effect is greater with low molecular weight PEGs. The flux increase is also more pronounced at low concentration: Flux values nearly vary as a linear function of decimal logarithm of the salt concentration. The increase in flux is accompanied by a decline in PEG retention.

These results, like those observed when the pH was varied, are in conflict with those reported in the literature. Mochizuki and Zydney (13) investigated the flux and the retention of dextran solutions over bovine serum albumin (BSA) deposits and found that the flux goes through a maximum and the retentions through a minimum at the isoelectric point in the absence of salt. Opong and Zydney (12) and Palecek, Mochizuki, and Zydney (14) showed that the permeability of the protein deposits decreased with increased solution ionic strength both above and below the protein isoelectric point but was relatively independent of ionic strength at the isoelectric point. They also showed that the fluxes and retentions through protein deposits change as a function of protein type and more precisely as a function of the protein charge density. In fact, the pH and ionic strength can affect the permeability of protein layers in three ways: 1) by modifying the electric charge and eventually the structure of the proteins, 2) by shielding the electrostatic re-

Downloaded At: 10:41 25 January 2011

Copyright © Marcel Dekker, Inc. All rights reserved.

MARCEL DEKKER, INC.
270 Madison Avenue, New York, New York 10016

ORDER REPRINTS

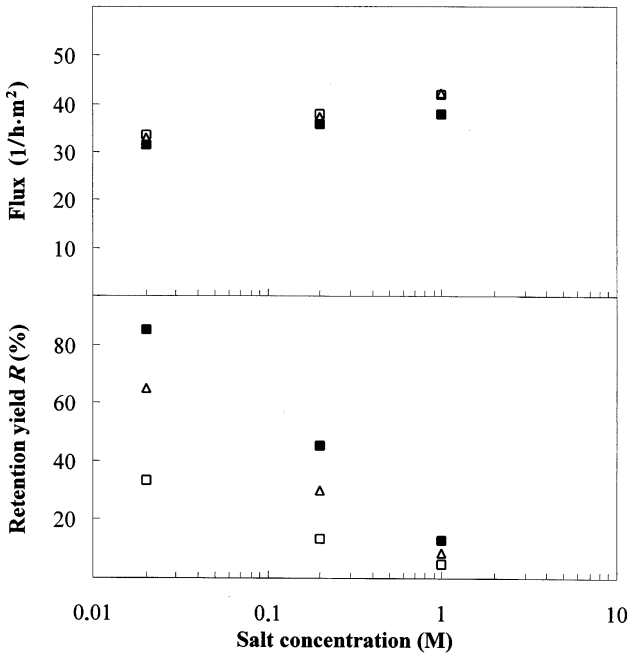

Figure 3. Flux and retention yields versus NaCl concentration (□ PEG 0.6 kd, △ PEG 1.5 kd, ■ PEG 6.0 kd).

pulsions between adjacent chains within the deposit, and 3) by modifying the electroosmotic counterflow generated by the streaming potential due to the flow of charged species.

At high salt concentrations, the effect of the electroosmotic counterflow is limited, which should result in increased permeation flow and decreased retention. Yet, the shield effect is maximized, and as a consequence the inter- and intramolecular electrostatic interactions between the protein molecules should be diminished resulting in increased retention and decreased permeate flow. According to Palacek and Zydney (15), the shielding effect would be the most important one and could explain the results that they observed. However, in our case, as the protein layer was stabilized by the linking agent (formaldehyde), the chains may not be able to get close to each other, and so the hydraulic permeability of the membrane is not reduced.

Furthermore, our protein membrane was obtained from gelatin deposit while Mochizuki and Zydney (13) studied the permeability of BSA layers. Gelatin is a very hydrophilic protein and presents a collagen-like configuration, and BSA is a globular protein stabilized by a very hydrophobic core and strong surface

Downloaded At: 10:41 25 January 2011

Copyright © Marcel Dekker, Inc. All rights reserved.

MARCEL DEKKER, INC.
270 Madison Avenue, New York, New York 10016

ORDER REPRINTS

charges; therefore, these two proteins form different types of gel layers when deposited on a membrane surface. The permeability of protein gel is closely linked to the morphology of the gel structure. A gel, whether created intentionally or formed inadvertently due to membrane fouling, could be considered a three-dimensional network of protein molecules with solvent entrapped in the meshes. Its morphology results from covalent links that form between the different polypeptide chains as well as from secondary forces. In the case of gelatin, intra- and interprotein interactions and protein-solvent interactions are mostly a result of hydrogen bonding (18). As a result, any change of pH or ionic strength in the protein environment affects the strength of the hydrogen-bonded links and modifies the structure and the permeability of the protein gel layer. Moreover, NaCl is known to destabilize gelatin structure (18). At higher salt concentrations, as a consequence of both the protein and salt competing for water hydration, the gel layer is dehydrated, thus leading to larger pore spaces and improved flux.

As shown in Table 4, the effect of ionic strength on membrane properties is irreversible at low PEG concentrations. The original retention of PEG 0.6 kd could not be recovered even though the membrane was rinsed with ultrapure water before being characterized. Nonetheless, with PEG 1.5 and 6.0 kd, membrane properties were recovered after an ultrapure water filtration when the NaCl concentration was lower than 0.2 mol/L. The ionic strength, as does the pH, modifies the membrane structure in an irreversible way.

Downloaded At: 10:41 25 January 2011

Membrane Transport Properties

The estimation of membrane transport parameters (L_p, ω, and σ) requires that one has a sufficient number of experimental values (J_s, R). Nakao and Kimura (4), as well as Sarrade, Rios, and Carles (5), followed permeate flux variations and retention as a function of transmembrane pressure and tangential velocity. In our case, to prevent any uncontrolled change of properties of the compressible protein layer, J_s and R were observed as a function of the PEG solution concentrations.

Table 4. Standardized Characterization of Protein Membrane Before and After Filtration of Solutions of Increased Ionic Strength

	Retention Yields (%)			
kd	Initial	After Filtration at 0.02 mol/L	After Filtration at 0.2 mol/L	After Filtration at 1 mol/L
PEG 0.6	50	45	31	24
PEG 1.5	75	70	64	55
PEG 6.0	91	91	93	86

Copyright © Marcel Dekker, Inc. All rights reserved.

MARCEL DEKKER, INC.
270 Madison Avenue, New York, New York 10016

ORDER REPRINTS

Filtration of Solutions at Different Concentrations

After hydration of the membrane by tangential circulation of ultrapure water for 1 hour, PEG 0.6, 1.0, and 1.5 kd at 15, 30, 45, 60, 75, 90, and 105 g/L were filtrated. For each type of solute, the model solutions were successively used in order by increased concentration. The pH of all the solutions was 6.5. The results are shown in Fig. 4. As polarization became more pronounced as the bulk concentration increases, fluxes decreased. This decline was accompanied by a decrease in observed retention (R).

Estimation of Transport Parameters

The mass transfer coefficient (k) and solute concentration at the membrane surface (C_m) are deduced from data points. The values of k, calculated from Eq. (2) with υ and D values that are shown in Table 1, are given in Table 5 along with

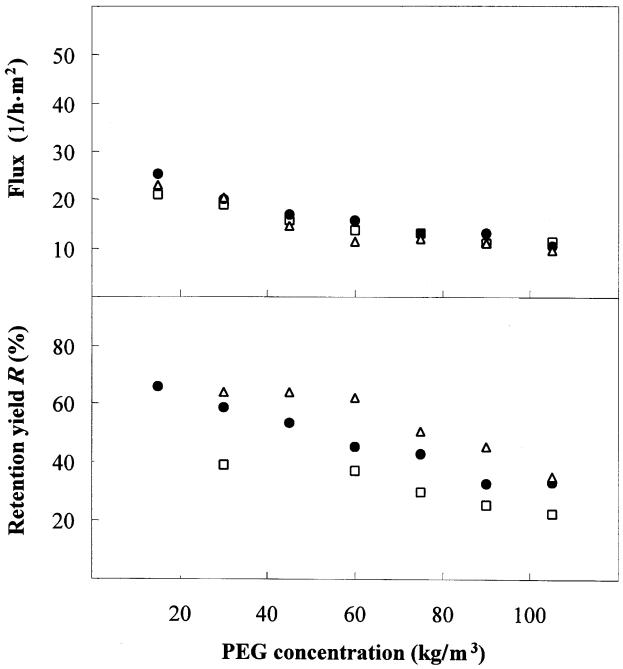

Figure 4. Flux and retention yields versus PEG concentrations (□ PEG 0.6 kd, ● PEG 1.0 kd, △ PEG 1.5 kd).

Downloaded At: 10:41 25 January 2011

Copyright © Marcel Dekker, Inc. All rights reserved.

MARCEL DEKKER, INC.
270 Madison Avenue, New York, New York 10016

ORDER REPRINTS

Table 5. Mass Transfer Coefficient, k (10^{-6} m/s[1]), and Polarization Layer Thickness, δ (10^{-5} m), at Variable Concentrations of PEGs

C_o (kg/m^3)	PEG 0.6 kd		PEG 1.0 kd		PEG 1.5 kd	
	k	δ	k	δ	k	δ
15	19.2	2.08	15.1	1.92	11.7	1.89
30	14.1	2.27	10.9	2.20	8.4	2.01
45	10.8	2.41	8.0	2.38	5.8	2.23
60	8.4	2.62	5.8	2.58	4.1	2.45
75	6.5	2.77	4.3	2.79	2.9	2.72
90	4.6	3.02	3.2	3.13	2.0	3.00
105	3.6	3.32	2.4	3.40	1.5	3.35

$U = 1$ m/s; $T = 293$ K; $\Delta P = 2 \times 10^5$ Pa.

the estimated thickness of the mass-transfer boundary layer δ. However, J_v and C_p data points as well as calculated C_m are reported in Table 6.

The permeability (L_p) of the protein membrane is determined by filtrating ultrapure water at different pressure gradients. From plots of J_v versus ΔP, L_p is estimated at 7×10^{-11} m/s·Pa. ω and σ can be estimated either from graphs of

$$\frac{J_s}{\Delta C} \text{ versus } C^*\left(\frac{J_v}{\Delta C}\right)$$

or from Eqs. (7) and (8). Both methods give consistent results for PEG 1.0 kd. However, these graphical interpretations led to suspect results for the other two PEGs: $\omega < 0$ for PEG 0.6 kd and $\sigma > 1$ for PEG 1.5 kd. These unexpected results

Table 6. Flux J_v (10^{-6} m/s), Permeate C_p (kg/m^3) and Surface C_m (kg/m^3) Concentrations

C_o (kg/m^3)	PEG 0.6 kd			PEG 1.0 kd			PEG 1.5 kd		
	J_v	C_p	C_m	J_v	C_p	C_m	J_v	C_p	C_m
15	5.83	N/A	N/A	7.00	5.43	20.6	6.42	N/A	N/A
30	5.25	18.8	35.1	5.83	12.9	42.0	5.83	8.97	50.9
45	4.38	30.2	52.4	4.67	21.6	63.5	3.50	13.8	70.7
60	4.08	39.5	72.8	4.08	32.7	87.7	2.92	19.8	101.8
75	3.79	55.7	90.2	3.50	45.3	112.3	2.92	33.1	146.3
90	3.21	71.1	108.2	3.60	59.8	152.6	2.33	44.0	191.6
105	3.50	88.7	131.6	2.33	69.3	165.4	1.93	61.8	219.3

N/A Data not available.

Downloaded At: 10:41 25 January 2011

Copyright © Marcel Dekker, Inc. All rights reserved.

ORDER REPRINTS

Table 7. Transport Parameter Values

	PEG 0.6 kd	PEG 1.0 kd	PEG 1.5 kd
Solute permeability ω (10^{-6} m/s)	2.466	1.134	0.394
Reflection coefficient σ	0.57	0.74	0.84
Solute rs (nm)	0.6	0.8	1.5
Calculated pore radii rp (nm)	1.309	1.392	1.504

probably are due to a low number of data points. Therefore, in Table 7 only the values estimated by calculation are indicated. The mean pore radius of the membrane was estimated through the use of Eqs. (10) and (11). Regardless of the PEG tested, the results are very close, ranging from 1.3 to 1.5 nm as seen in Table 7. The use of this kind of model should be questioned because the model is based on the assumption that the membrane is a network containing fixed water-filled cylindrical channels/pores through which mass transport occurs. However, Kra-

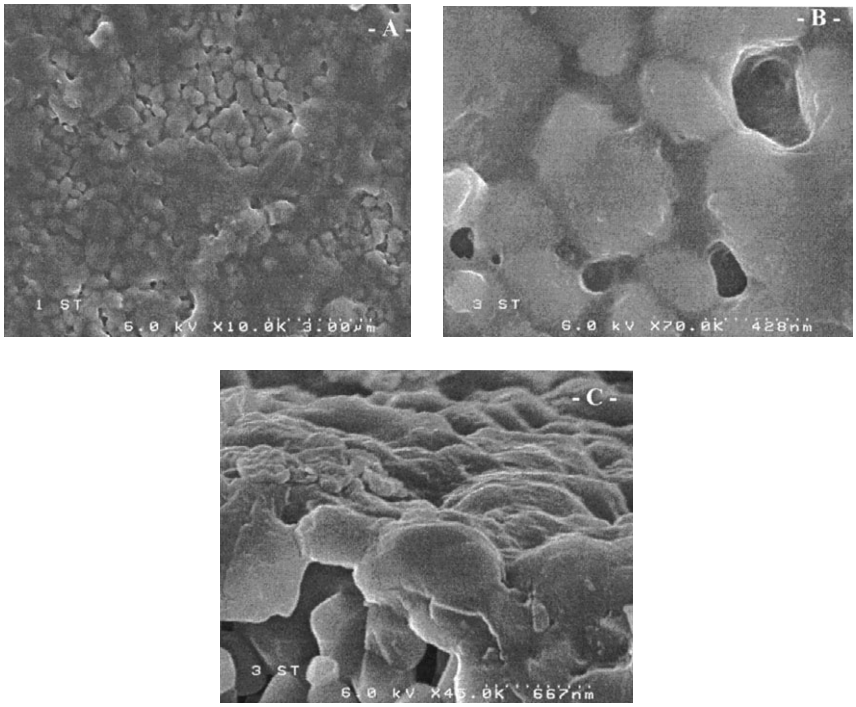

Figure 5. SEM photographs for a standard proteinic membrane (A) surface layer, (B) details, and (C) transversal cut.

Downloaded At: 10:41 25 January 2011

Copyright © Marcel Dekker, Inc. All rights reserved.

MARCEL DEKKER, INC.
270 Madison Avenue, New York, New York 10016

ORDER REPRINTS

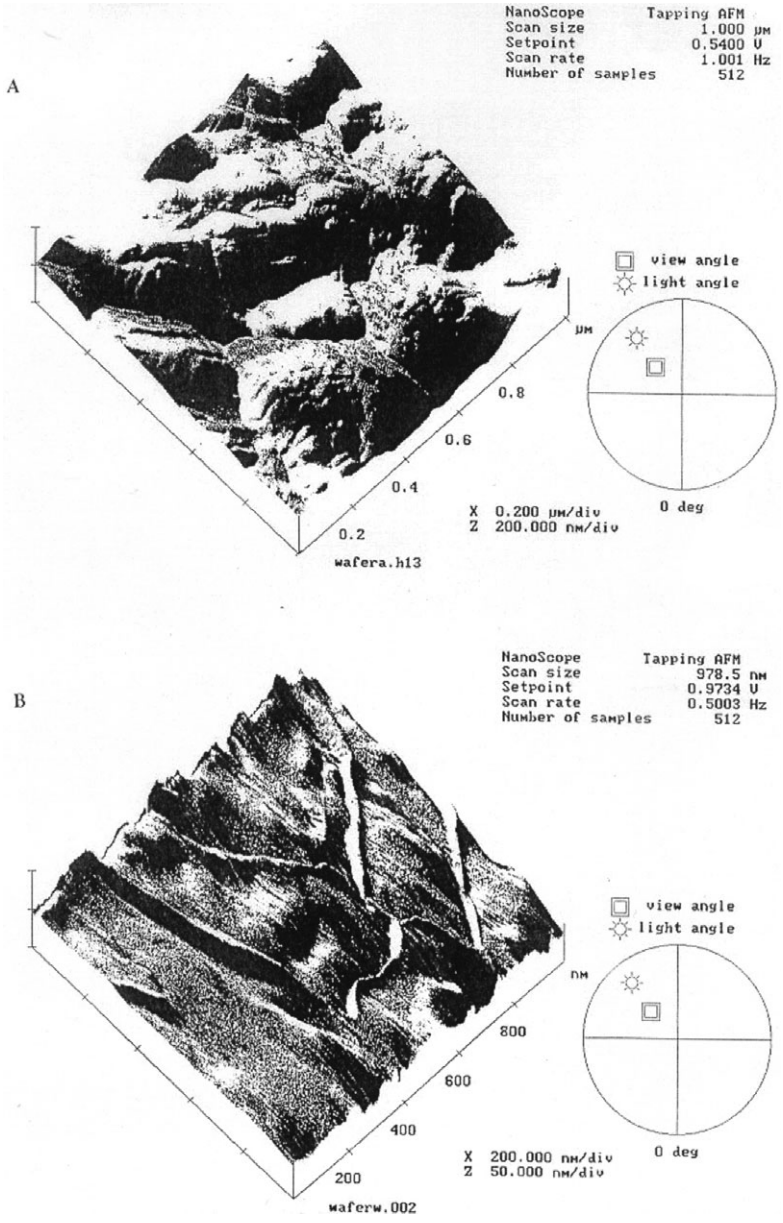

Figure 6. AFM images of a standard gelatin membrane (A) dried and (B) wet.

Downloaded At: 10:41 25 January 2011

Copyright © Marcel Dekker, Inc. All rights reserved.

ORDER REPRINTS

jewska and Olech (19–20), who used that model to determine the pore radii of membranes created from chitosan, found results consistent with those obtained in 2 other ways.

Physical Characterization of the Membrane

Figure 5 exhibits SEM photographs for a standard gelatin membrane. Photograph 5A reveals that the gelatin layer is not uniform. In some zones, the protein deposit seems denser than in others areas; the alumina support can even be observed in places. The photograph 5B focuses on a defect of the protein layer. The protein penetrates inside the support, but the bottom cannot be checked to determine if it is covered with gelatin. In picture 5C a transversal cut of the membrane is shown, and a superficial gelatin deposit can be observed. Its thickness is too thin to be estimated.

Figure 6 shows the topographies obtained by AFM of a standard gelatin membrane. Figure 6A shows the dried membrane while Fig. 6B shows a membrane that was submerged in water for 6 hours. Figure 6A allowed us to characterize the surface of the ceramic support under the gelatin deposit. The protein deposit takes the shape of the alumina grains, and the depressions observed probably correspond to the entry of the pores of the inorganic support. Figure 6B shows an aspect of the membrane closer to reality because the image was obtained under wet conditions: The protein layer appears more hydrated, more swollen, in Fig. 6B than in Fig. 6A. The surface observed in Fig. 6B is more uniform than that of Fig. 6A, and the depressions observed in Fig. 6A seem less deep than those of Fig. 6B. The openings of support pores are partially filled in Fig. 6B, which explains why the selectivity of protein layer is better than that of the ceramic support alone. Contrary to other results already described in the literature (21–23), which report on AFM applications for microfiltration membrane characterization, we could not estimate the pore size of the deposited layer. However, the channels, at the bottom of which the solute may cross the membrane, are not cylindrical (as proposed in the model described above) but are in the form of valleys.

CONCLUSION

In this paper, we present our studies on the structure and the transport properties of a protein membrane. The SEM observations showed that the gelatin forms an ultrathin layer over the surface of a ceramic support. The AFM permitted the observation of the wet layer. The size reduction of support pores, filled with a swollen gelatin layer, could explain the selectivity of the protein membrane. The use of a mass transfer model, even if a few simplifying assumptions are applied to it, permit the estimation of a mean pore diameter between 2.6 and 3.0 nm.

Downloaded At: 10:41 25 January 2011

Copyright © Marcel Dekker, Inc. All rights reserved.

MARCEL DEKKER, INC.
270 Madison Avenue, New York, New York 10016

ORDER REPRINTS

Filtration experiments performed at various pH and ionic strengths showed that the macromolecular deposit structure is strongly dependent on these two parameters. High and small pH values and high ionic strengths increase the permeability of the membrane and reduce its selectivity. These modifications are partially irreversible. An in-depth understanding of gelatin solution behavior (intraprotein, interprotein, and protein-solvent interactions) is necessary for a better understanding of the permeability of the deposited layer. However, the lack of information on the far less-known interactions that are responsible for fixing proteins onto the inorganic surface (such as, their nature and relative strength) and that narrowly condition the whole structure of the deposited layer prohibits a thorough explanation of gel protein morphology and resulting transport phenomena.

Downloaded At: 10:41 25 January 2011

NOMENCLATURE

C^*	mean concentration over the membrane thickness (kg/m^3)
C_m	solute concentration at the membrane surface (kg/m^3)
C_o	solute concentration in feed stream (kg/m^3)
C_p	solute concentration in permeate (kg/m^3)
C_r	solute concentration in retentate (kg/m^3)
D	diffusion coefficient (m^2/s)
J_v	solvent flux ($l/h \cdot m^2$)
J_s	solute flux ($mol/m^3 \cdot s$)
k	mass transfer coefficient (m/s)
L_p	pure water permeability ($m/s \cdot Pa$)
M.W.	molecular weight (dalton)
q	ratio of solute radius to membrane pore radius (r_s/r_p)
R^*	real retention (%)
R	observed retention (%)
Re	Reynolds number
r_p	pore radius (m)
r_s	Stokes-Einstein radius (m)
Sc	Schmidt number
Sh	Sherwood number
U	tangential fluid velocity (m/s)

Greek Symbols

δ	boundary-layer thickness (m)
$\Delta\Pi$	osmotic pressure (Pa)
ΔP	transmembrane pressure (Pa)

Copyright © Marcel Dekker, Inc. All rights reserved.

MARCEL DEKKER, INC.
270 Madison Avenue, New York, New York 10016

ORDER REPRINTS

σ reflection coefficient (−)
υ kinematic viscosity (m^2/s)
ω solute permeability (m/s)

ACKNOWLEDGMENTS

The authors wish to acknowledge Professors A. Cardenas, O. Rojas, and J-L. Salager of the Universidad de Los Andes for their help. The stay in France of one of the authors (J. Bullón) was made possible by a CONICIT-Venezuela (Universidad de Los Andes) scholarship and by the French-Venezuelan cooperative program PCP "Surfactants and Applications."

Downloaded At: 10:41 25 January 2011

REFERENCES

1. Negrel, J.L.; Rios, G.M.; Cuq, J.L. Membranes Organo-inorganiques Obtenues par Dépôt de Protéines sur un Support Macroporeux. French patent 96.01733, February 13, 1996.
2. Negrel, J.L.; Belleville, M.P.; Rios, G.M. Newly-Designed Proteinic Membrane for Low Ultrafiltration. J. Membr. Sci. **1997,** *134* (2), 163–170.
3. Bullón, J.; Belleville, M.P.; Rios, G.M. Preparation of Gelatin Formed-in-Place Membranes: Effect of Working Conditions and Substrates. J. Membr. Sci. **2000,** *168* (2), 159–165.
4. Nakao, S.; Kimura, S. Analysis of Solutes Rejection in Ultrafiltration. J. Chem. Eng. Jpn. **1981,** *14* (1), 32–37.
5. Sarrade, S.; Rios, G.M.; Carles, M. Dynamic Characterization and Transport Mechanisms of Two Inorganic Membranes for Nanofiltration. J. Membr. Sci. **1994,** *97*, 155–166.
6. Michaels, A.S. New Separation Technique for the Chemical Process Industries. Chem. Eng. Prog. **1968,** *64*, 31–43.
7. Porter, M.C. Concentration Polarization with Membrane Ultrafiltration. Ind. Eng. Chem. Prod. Res. Develop. **1972,** *11* (3), 234–248.
8. Deissler, R.G. *Analysis of Turbulent Heat Transfer, Mass Transfer and Friction in Smooth Tubes at High Prandtl and Schmidt Numbers*, NACA Report, No. 1210,1955.
9. Pappenheimer, J.R.; Renkin, E.M.; Borrero, J.P. Filtration, Diffusion and Molecular Sieving Through Peripheral Capillary Membranes (A Contribution to the Pore Theory of Capillary Permeability. Am. J. Physiol. **1951,** *167*, 13–46.
10. Verniory, A.R.; Du Bois, R.; Decoodt, P.; Gassée, J.P.; Lambert, P.P. Measurement of the Permeability of Biological Membranes—Application to the Glomerular Wall. J. Gen. Physiol. **1973,** *62,* 489–507.

Copyright © Marcel Dekker, Inc. All rights reserved.

MARCEL DEKKER, INC.
270 Madison Avenue, New York, New York 10016

ORDER REPRINTS

11. Marshall, A.D.; Munro, P.A.; Tragardh, G. The Effect of Protein Fouling in Microfiltration and Ultrafiltration on Permeate Flux, Protein Retention and Selectivity: A Literature Review. Desalination **1993,** *91* (1), 65–108.
12. Opong, W.S.; Zydney, A.L. Hydraulic Permeability of Protein Layers Deposited During Ultrafiltration. J. Colloid Interface Sci. **1991,** *142* (1), 41–60.
13. Mochizuki, S.; Zydney, A. Sieving Characteristics of Albumin Deposits Formed During Microfiltration. J. Colloid Interface Sci. **1993,** *158*, 136–145.
14. Palecek, S.P.; Mochizuki, S.; Zydney, A.L. Effect of Ionic Environment on BSA Filtration and the Properties of BSA Deposits. Desalination **1993,** *90*, 147–159.
15. Palecek, S.P.; Zydney, A.L. Hydraulic Permeability of Protein Deposits Formed During Microfiltration: Effect of Solution pH and Ionic Strength. J. Membr. Sci. **1994,** *95,* 71–81.
16. Huisman, I.H.; Prádanos, P.; Hernández, A. The Effect of Protein-Protein and Protein-Membrane Interactions on Membrane Fouling in Ultrafiltration. J. Membr. Sci. **2000,** *179* (1), 79–90.
17. Ward, A.G.; Courts, A. The Science and Technology of Gelatin; Academic Press: London, 1977; 179–294.
18. Eysée-Collen, B.; Lencki, R.W. Protein Ternary Phase Diagrams. I. Effect of the Ethanol, Ammonium Sulfate, and Temperature on the Phase Behavior of the Type B Gelatin. J. Agr. Food Chem. **1996,** *44,* 1651–1657.
19. Krajewska, B.; Olech, A. Pore Structure of Gel Chitosan Membranes. I. Solute Diffusion Measurements. Polym. Gels Netw. **1996,** *4*, 33–43.
20. Krajewska, B. Pore Structure of Gel Chitosan Membranes. III. Pressure-Driven Mass Transport Measurements. Polym. Gels Netw. **1996,** *4,* 55–63.
21. Bessières, A.; Meireles, M.; Coratger, R.; Beauvillanin, J.; Aimar, P.; Sanchez, V. Study of Surface Topography and Pore Structure of Polymeric Membranes with Near Field Microscopy (AFM and STM), Euromembranes '95, Bath, UK, Sept. 18–20, 1995.
22. Bowen, W.R.; Hilal, N.; Lovitt, R.W.; Williams, P.M. Visualisation of an Ultrafiltration Membrane by Non-Contact Atomic Force Microscopy at Single Pore Resolution. J. Membr. Sci. **1996,** *110* (2)*,* 229–232.
23. Bowen, W.R.; Hilal, N.; Lovitt, R.W.; Williams, P.M. Atomic Force Microscope Studies of Membranes: Surface Pore Structure of Cyclopore and Anopore Membranes. J. Membr. Sci. **1996,** *110 (*2), 233–238.

Received August 2000
Revised January 2001

Downloaded At: 10:41 25 January 2011

Copyright © Marcel Dekker, Inc. All rights reserved.

MARCEL DEKKER, INC.
270 Madison Avenue, New York, New York 10016

Downloaded At: 10:41 25 January 2011

Request Permission or Order Reprints Instantly!

Interested in copying and sharing this article? In most cases, U.S. Copyright Law requires that you get permission from the article's rightsholder before using copyrighted content.

All information and materials found in this article, including but not limited to text, trademarks, patents, logos, graphics and images (the "Materials"), are the copyrighted works and other forms of intellectual property of Marcel Dekker, Inc., or its licensors. All rights not expressly granted are reserved.

Get permission to lawfully reproduce and distribute the Materials or order reprints quickly and painlessly. Simply click on the "Request Permission/Reprints Here" link below and follow the instructions. Visit the U.S. Copyright Office for information on Fair Use limitations of U.S. copyright law. Please refer to The Association of American Publishers' (AAP) website for guidelines on Fair Use in the Classroom.

The Materials are for your personal use only and cannot be reformatted, reposted, resold or distributed by electronic means or otherwise without permission from Marcel Dekker, Inc. Marcel Dekker, Inc. grants you the limited right to display the Materials only on your personal computer or personal wireless device, and to copy and download single copies of such Materials provided that any copyright, trademark or other notice appearing on such Materials is also retained by, displayed, copied or downloaded as part of the Materials and is not removed or obscured, and provided you do not edit, modify, alter or enhance the Materials. Please refer to our Website User Agreement for more details.

Order now!

Reprints of this article can also be ordered at
http://www.dekker.com/servlet/product/DOI/101081SS100107760